Oxide interfaces with enhanced ion conductivity

Carlos Leon, Jacobo Santamaria, and Bernard A. Boukamp

The new field of nano-ionics is expected to yield large improvements in the performance of oxide-based energy generation and storage devices based on exploiting size effects in ion conducting materials. The search for novel materials with enhanced ionic conductivity for application in energy devices has uncovered an exciting new facet of oxide interfaces. With judicious choice of the constituent materials, oxide heterostructures can exhibit enhanced ion mobility compared to the bulk counterparts. Here we review recent experimental and theoretical progress on enhancement of oxide-ion conductivity arising in oxide ultrathin layers and at their interfaces, and describe the different scenarios, space-charge effects, epitaxial strain, and atomic reconstruction at the interface, proposed to account for the observed conductivity enhancement.

Introduction

The recent surge of interest in oxide interfaces has been fueled by the possibility of stabilizing electronic ground states, leading to emerging properties. Many of these complex oxides share a common perovskite structure with similar lattice parameters that allow the growth of epitaxial interfaces with high structural perfection. At interfaces, electron correlations establish novel forms of coupling between electronic ground states of the adjoining materials, which have been proposed to be the origin of emergent properties.[1] A paradigmatic case is the metallic state at the interface between two band insulators as in LaAlO$_3$/SrTiO$_3$ (LAO/STO) heterostructures.[2] This finding triggered a new research field aimed at finding interesting novel phases at oxide interfaces with a high potential for applications.[3–5]

At interfaces, the important quantities controlling the nucleation of different electronic phases (charge density, electrostatic repulsion and bandwidth) may change substantially in a phenomenon called electronic reconstruction.[6,7] In addition, interface strain is also an important parameter controlling phase stabilization.[8–13] Oxides, as compared to other materials, are able to accommodate very large amounts of epitaxial strain without breaking into islands or structural domains. This is probably due to the large polarizability of the oxygen sublattice,[7] which admits quite large deformations in the form of rotations and distortions of the oxygen octahedra.

The possibility of tailoring electronic properties at oxide interfaces has raised the question of whether the properties of oxygen ion conducting materials could also be modified at interfaces. In this regard, the coherent growth of strained interfaces in heterostructures combining materials with different degrees of lattice mismatch has been shown to promote ion diffusivity[14] and thus, these heterostructures may play an important role in the optimization of materials for electrochemical devices such as batteries and fuel cells that are key to commercially viable low power energy generation and storage.[15,16] In particular, enhanced oxide-ion conductivity at oxide interfaces would be relevant for lowering the operation temperature of solid oxide fuel cells (SOFCs). In SOFCs, O^{2-} ions form at the cathode and diffuse through a solid electrolyte material at elevated temperatures (usually 800–1000°C) to react with H$^+$ ions in the anode to produce water. The high operation temperatures favor internal fuel reformation, electrode processes, and ionic migration through the electrolyte, but impose serious restrictions on materials selection due to thermal stress or fatigue. Thus, a major materials research goal today is to reduce the operating temperature of SOFCs without compromising device performance.[15] Novel electrolytes are needed with higher oxide-ion conductivity and also electrode materials with higher oxygen exchange rates.

Carlos Leon, Department of Applied Physics, Universidad Complutense, Madrid; carlos.leon@fis.ucm.es
Jacobo Santamaria, Applied Physics Department, Universidad Complutense, Madrid; jacsan@fis.ucm.es
Bernard A. Boukamp, University of Twente, The Netherlands; b.a.boukamp@utwente.nl

Materials synthesis strategies based on chemical substitutions to increase the concentration of mobile species have limitations, and increasing conductivity beyond the values corresponding to optimal concentrations requires increasing the operation temperature.[16–18] A different strategy to find materials with higher ionic conductivity is to exploit the conductivity increases that result from size effects, when (one or more) sample dimensions are reduced down to the nanometer scale. Nanotechnology is expected to have a large impact on the next generation of fuel cells since ionic transport can be strongly modified in nanomaterials.[19–21] The term nano-ionics has been coined to embrace the new concepts in ion transport and electrochemical storage resulting from nanoscale effects.[22]

In this article, we review recent results of enhanced oxygen ion conductivity at oxide interfaces as well as the theoretical scenarios being considered to explain it. In particular, space-charge effects, which might account for changes in the carrier density, and epitaxial strain, which might tailor an enhanced mobility pathway for the ions, are revised. The atomic reconstruction occurring at interfaces between complex oxides is also discussed as a source of unexpected changes in the interface chemistry, where the mismatch in the bonding or polar structure of the layers might play a leading role. A final section is devoted to oxygen surface exchange, which may also be strongly enhanced at interfaces, signaling a new route toward novel artificial electrode materials in solid oxide fuel cells.

Space-charge effects

It is well established that the energy required for defect generation may be different at surfaces or boundaries. The discontinuity of free energy at interfaces naturally results in charge transfer processes that break charge neutrality and may profoundly change the carrier density. In ionic compounds, the accumulation of defects creates an electric field that is screened over a space-charge layer (the spatial extent of the electric field), by depletion or accumulation of mobile charges, and whose characteristic length scale is the Debye length, the length scale of charge inhomogeneities.[23] Space-charge effects are known to give rise to interesting nano-ionic size effects emerging when the extension of the space-charge region is comparable to sample dimensions.[24–26] Quite remarkable is the large enhancement of the electronic conductivity discovered in mixed ionic-electronic conductor CeO_2 nanocrystalline samples, in the pioneering work by Tuller and co-workers, measured by impedance spectroscopy and discussed in terms of accumulation of vacancies at the grain boundary cores.[27] Maier and colleagues[28] have broken new ground in nano-ionics, showing a large increase in ionic conductivity in layered thin-film BaF_2/CaF_2 superlattices as a result of an interfacial effect resulting from the transfer of fluorine ions into the CaF_2 side due to the electrochemical potential gradient across the interface. This yields enhanced vacancy concentration in the Ba side when the thickness of the individual layers become comparable to the size of the space-charge region (i.e., of tens of nanometers).

Following the work by Maier et al., there were some controversial results on the occurrence of space-charge effects at the interfaces of oxide-ion conductors, such as yttria-stabilized zirconia (YSZ), x Y_2O_3: $(1–x)$ ZrO_2. Among oxide-ion conductors, those of the anion-deficient fluorite structure such as YSZ are extensively used today as electrolytes in SOFCs.[15,17] Doping with Y_2O_3 is known to stabilize the cubic fluorite structure of ZrO_2 at room temperature and simultaneously supply oxygen vacancies responsible for its ionic conductivity.[18] Some authors reported increases in ionic conductivity in nano-granular samples,[29] while others found no changes[30] or even decreases[31,32] in conductivity.[18] O tracer diffusion experiments assisted by secondary ion mass spectroscopy also yielded contradictory results: While a three orders of magnitude increase in the diffusion coefficient as compared with bulk samples was reported in nanocrystalline thin films,[33] bulk nanocrystalline ceramics showed no change.[34]

It was also not straightforward to explain the observed increases due to a space-charge effect, because the Debye screening length in these materials is very short, on the order of 0.1 nm for typical dopant concentrations (8% YSZ) at intermediate temperatures (500°C). However, the possibility of enhanced ionic conductivity in nanostructures triggered large activity in the field, mainly due to its impact in the design of electrolytes with lower operation temperatures[35] or in electrodes with higher oxygen exchange rates.[36] Tuller and colleagues[37] found a two orders of magnitude increase in the high temperature ionic conductivity of thin films of YSZ deposited by spin coating on Al_2O_3 when their thickness was reduced to the 10 nm range.

Later, Kosacki et al.[38] also reported a large increase in the conductivity of 10% Y_2O_3 doped YSZ epitaxial thin films grown on MgO when thickness was reduced down to 15 nm. The conductivity increase, of more than two orders of magnitude at 400°C, was accompanied by a reduction in the activation energy down to 0.62 eV. The authors attribute the conductivity increase to a highly conducting 1 nm layer at the YSZ/MgO interface. Karthikeyan et al.[39] found a more moderate conductivity increase of one order of magnitude for 17-nm-thick YSZ polycrystalline multiphase samples grown on MgO.

On the other hand, Guo et al.[40] found a decrease in the ionic conductivity of 12-nm-thick nanostructured polycrystalline YSZ thin films deposited on MgO as compared to 8% Y_2O_3 doped bulk ceramics and essentially no change in the activation energy, suggesting that epitaxial growth is an important step in attaining enhanced ionic mobility. In fact, a number of papers have reported increased conductivity of fluorite-based heterostructures and superlattices associated with the increased migration volume resulting from misfit dislocations at the interface.[41–44] This indicated that enhanced conductivity at epitaxial interfaces involving nanometer-thick YSZ may arise not only from space-charge effects but also from epitaxial strain or atomic reconstruction reported to appear at interfaces between correlated oxides.[45,46]

Epitaxial strain

Motivated by these previous reports, and in an attempt to isolate a true interface effect on ion conductivity in oxide heterostructures, Garcia-Barriocanal et al.[14] grew highly strained multilayers combining STO and ultrathin YSZ layers with controlled thickness down to the unit cell level (0.3–1 nm) (see **Figure 1**). They found conductivity values from dielectric spectroscopy measurements as large as eight orders of magnitude higher than bulk YSZ conductivity values at room temperature, which they attributed to enhanced oxide-ion conductivity.[14] The DC conductivity determined from the low frequency plateau of conductivity spectra was independent of the YSZ layer thickness, which was taken as an indication of its interfacial origin.

Guo has proposed[47] the electronic origin of the large conductivity values found in this experiment, but the possibility that the enhanced conductivity originated in electron doping of the substrate or STO layers was eliminated by measuring the DC (electronic) contribution of the conductivity, which turned out to be almost three orders of magnitude smaller than the global conductivity measured with AC methods.[48] DC ionic conductivity is thermally activated according to the following expression,
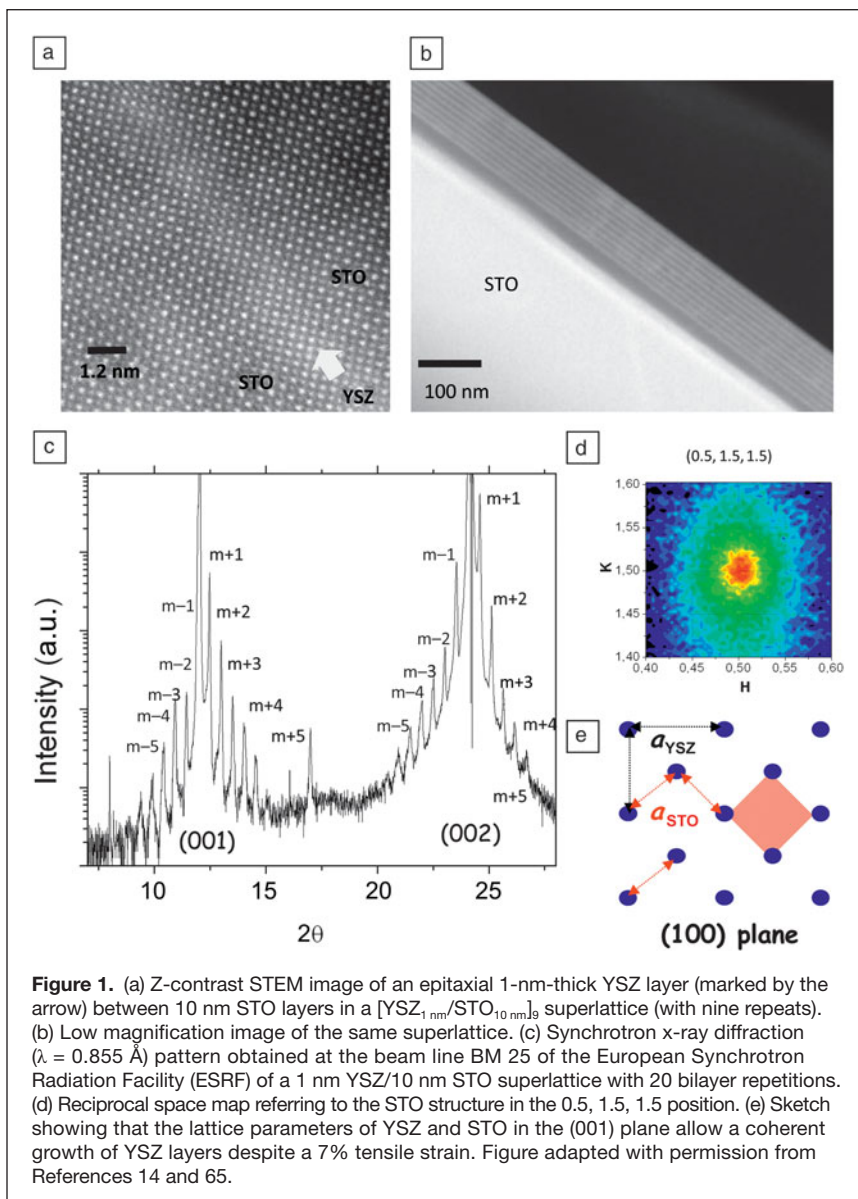
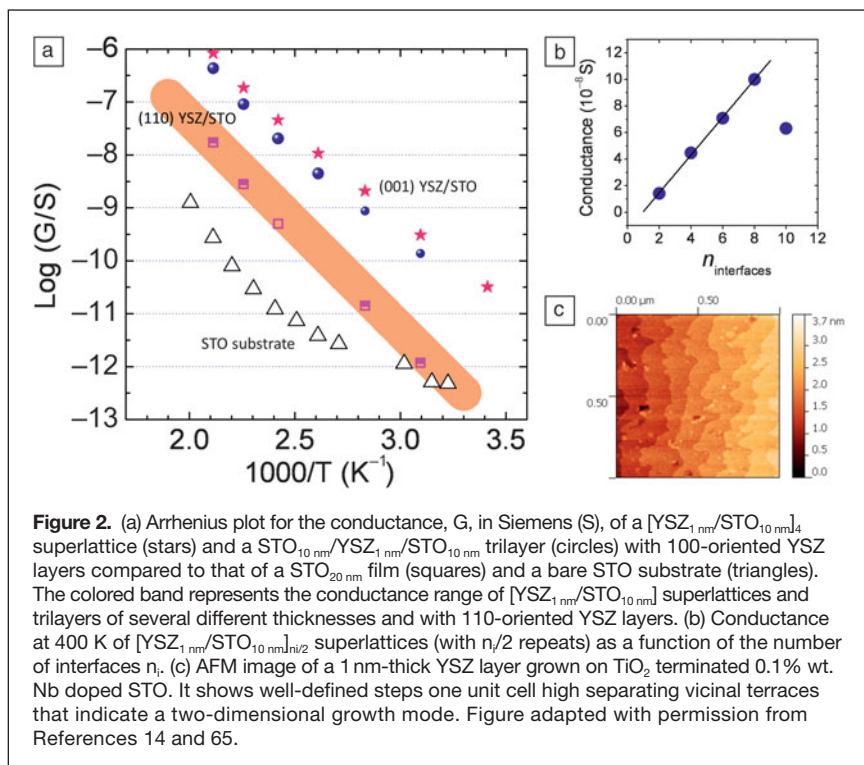$$\sigma_{dc} = \frac{4\alpha e^2 a^2 \nu_0 N e^{S/k_B}}{k_B} e^{-E_A/k_B T} \qquad (1)$$

where α is a geometrical factor, a is the jump distance, ν_0 is the attempt frequency, N is the concentration of oxygen vacancies, S is a configurational entropy term, e is the electron charge, k_B is the Boltzmann constant, and E_A is the activation energy. Garcia-Barriocanal et al.[14] discussed the conductivity enhancement in terms of a decrease in the activation energy from values of about 1 eV for bulk samples to 0.6 eV for ultrathin trilayers (see **Figure 2**a) and of the large conductivity pre-exponential factor of the STO/YSZ/STO trilayer samples, which may result from an increase in the concentration of oxygen vacancies, and/or a large entropy term related to disorder.[49]

A reduction in the activation energy for oxygen ion diffusion has been obtained from an *ab initio*-based kinetic Monte Carlo model for ionic conductivity in YSZ.[50] Ionic interactions are found to be essential to reproduce the effective activation energy,[51] and the enhanced oxygen ion mobility may result from a non-random distribution of dopant Y ions at the interfacial planes,[50] structural disorder,[52] or from a decrease in ionic interactions when the layer thickness goes down to the nanometer range.[53] An important point might be the effect of epitaxial strain on defect association, which in YSZ is known to immobilize oxygen vacancies at temperatures lower than 1000 K. Hence, the conductivity is controlled by both the mobility and the defect association constant. Generally, it is believed that associates are formed between yttrium in zirconium sites and oxygen vacancies (Y_{zr}' and $V_o^{..}$ in Kröger–Vink notation), although oxygen vacancies could also be immobilized by a strain field due to the size difference between Zr^{4+} and Y^{3+} cations.[54] An interesting possibility is that the apparent mobility could increase significantly when this strain field is alleviated by an externally induced strain (although not by several orders of magnitude).

Other authors have also reported substantial enhancement of the ionic conductivity (though smaller than in Reference 14) in ultrathin epitaxial YSZ layers. Sillassen et al.[55] reported a

Figure 1. (a) Z-contrast STEM image of an epitaxial 1-nm-thick YSZ layer (marked by the arrow) between 10 nm STO layers in a [YSZ$_{1 nm}$/STO$_{10 nm}$]$_9$ superlattice (with nine repeats). (b) Low magnification image of the same superlattice. (c) Synchrotron x-ray diffraction (λ = 0.855 Å) pattern obtained at the beam line BM 25 of the European Synchrotron Radiation Facility (ESRF) of a 1 nm YSZ/10 nm STO superlattice with 20 bilayer repetitions. (d) Reciprocal space map referring to the STO structure in the 0.5, 1.5, 1.5 position. (e) Sketch showing that the lattice parameters of YSZ and STO in the (001) plane allow a coherent growth of YSZ layers despite a 7% tensile strain. Figure adapted with permission from References 14 and 65.

Figure 2. (a) Arrhenius plot for the conductance, G, in Siemens (S), of a [YSZ$_{1\,nm}$/STO$_{10\,nm}$]$_4$ superlattice (stars) and a STO$_{10\,nm}$/YSZ$_{1\,nm}$/STO$_{10\,nm}$ trilayer (circles) with 100-oriented YSZ layers compared to that of a STO$_{20\,nm}$ film (squares) and a bare STO substrate (triangles). The colored band represents the conductance range of [YSZ$_{1\,nm}$/STO$_{10\,nm}$] superlattices and trilayers of several different thicknesses and with 110-oriented YSZ layers. (b) Conductance at 400 K of [YSZ$_{1\,nm}$/STO$_{10\,nm}$]$_{ni/2}$ superlattices (with n$_i$/2 repeats) as a function of the number of interfaces n$_i$. (c) AFM image of a 1 nm-thick YSZ layer grown on TiO$_2$ terminated 0.1% wt. Nb doped STO. It shows well-defined steps one unit cell high separating vicinal terraces that indicate a two-dimensional growth mode. Figure adapted with permission from References 14 and 65.

the measured mean oxygen ion diffusion coefficient versus layer thickness between 12 and 45 nm, they estimated an elastically strained interface region thinner than 5 nm with modified ionic transport properties.

One has to be careful interpreting impedance measurements when using active electrodes such as Ag or Pt. Gold is a better option to block oxygen ions.[61] Furthermore, surface diffusion (conduction) could influence measurement of the in-plain conductivity of thin films. The critical point about enhanced oxygen-ion conductivity is proven by ^{18}O-exchange experiments, preferably under current flow. There are also some controversial results regarding conductivity enhancement of epitaxially strained layers. Pergolesi et al.[62] studied YSZ-CeO$_2$ heterostructures on MgO substrates, where interfaces were found to be non-uniformly but significantly strained, and they reported no detectable contribution to the total conductivity even in the case of layers as thin as about 10 unit cells. Fleig et al.[63] grew, by using PLD, YSZ layers with larger thickness ranging from 30 to 300 nm onto MgO, Al$_2$O$_3$, and SrTiO$_3$ substrates with different lattice parameters, and they did not find an enhancement in ionic conductivity. They attribute this result to the presence of grain boundaries in the films that strongly block ion transport. Cavallaro et al.[64] have grown YSZ/STO heterostructures using PLD and found that the layers were discontinuous, and YSZ islands had mixed crystalline orientations. They found enhanced values of the electronic conductivity that they attributed to an interfacial alloyed oxide resulting from zirconium/strontium intermixing. These results suggest the possible importance of crystalline orientation of the YSZ growth in order to obtain coherent, epitaxial films with enhanced ionic conductivity.

By using different temperatures during the growth of YSZ films on STO using a sputtering technique, Rivera-Calzada et al.[65] were able to control the crystalline orientation that allowed stabilizing different morphologies, layer continuity, and epitaxy and, as a result, different degrees of ion mobility enhancement (see Figure 2). ⟨001⟩ YSZ growth yields coherent interfaces despite the 7% mismatch between the two highly dissimilar structures, stabilizing a disordered oxygen sublattice with an increased number of accessible positions for oxygen that promote oxygen diffusion. On the other hand, the ⟨110⟩ YSZ orientation results in the growth of connected islands, whose boundaries block the long range diffusion of ions. Moreover, conductance of superlattices with coherent interfaces scaled with the number of interfaces and is evidence that enhancement of ion conductivity is an interfacial effect (see Figure 2). These results show that epitaxial strain is an important parameter in designing a high mobility landscape at interfaces in addition to space-charge effects.[66,67]

more than three orders of magnitude enhancement of oxide-ion conductivity at low temperatures (lower than 350°C) in epitaxial YSZ films grown on MgO substrates. Their results also indicate that the observed enhancement is due to an interfacial effect and related to a combination of misfit dislocation density and elastic strain in the interface. The importance of epitaxial strain in determining the increase in ionic conductivity at oxide interfaces and nanolayers has been very recently addressed experimentally by several groups. Janek et al.[56] reported on the influence of strain on ion conduction at oxide interfaces, finding small conductivity enhancements in pulsed laser deposition (PLD) grown samples with partially coherent or non-coherent interfaces. Hertz et al.[57] have reported improved oxide-ion conductivity in ultrathin films of YSZ (below 10 nm thickness) grown by sputtering on Al$_2$O$_3$ substrates. There is an increase in the out-of-plane lattice parameter in these films due to tensile strain, which may assist in-plane ionic conduction. Lian et al.[58] have reported a two orders of magnitude increase in oxide-ion conductivity, as compared with bulk YSZ, in YSZ/Gd$_2$Zr$_2$O$_7$ heterostructures with 3% tensile strain and dislocation-free interfaces upon the manipulation of the layer thickness down to 5 nm.

Hyodo et al.[59] studied Pr$_2$Ni$_{0.71}$Cu$_{0.24}$Ga$_{0.05}$O$_4$/Sm$_{0.2}$Ce$_{0.8}$O$_2$ layer-by-layer nano-sized laminated films and found a significant increase in oxide-ion conductivity compared to values for bulk samarium doped ceria (SDC); they proposed this to be due to the expanded lattice of SDC in these heterostructures. Janek et al.[60] have reported an enhancement of [18]O tracer diffusion coefficient for transport along strained YSZ films in YSZ/Y$_2$O$_3$ multilayer samples. From the functional course of ent lattice parameters, and they did not find an enhancement

In fact, several theoretical groups have proposed that epitaxial strain provides an avenue to increase the conductivity of ion-conducting solids, and understanding its effects and uncovering the microscopic mechanism has become an important challenge.[53,56,68–74] One important direction has been the use of static models to evaluate changes in the migration volume. Korte and co-workers, using a qualitative model of ion diffusion along heterointerfaces based on the increased activation volume associated with the density of misfit dislocations and interfacial strain, have pointed out that strain by itself can only account for two to three orders of magnitude conductivity increase in YSZ/STO heterostructures.[56,68] This model predicts a linear increase of the conductivity with lattice mismatch for tensile strained interfaces, while compressive strain will decrease the ionic conductivity.

On the other hand, de Souza and colleagues[72,73] made use of static lattice simulation techniques using phenomenological potentials to describe the long range Coulomb interaction and the short range forces arising from electron cloud overlap. Lattice relaxation is performed over several hundreds of neighboring ions surrounding the migrating species. The effect of strain affects the free energy for migration through its effect on the free migration volume. This model would account for a conductivity increase up to five orders of magnitude using the experimental values of the activation energy in YSZ/STO heterostructures by Garcia-Barriocanal et al.[14] It is concluded that lattice strain alone cannot be responsible for the total conductivity increase found experimentally.[72] Furthermore, a recent paper by Yildiz and collaborators[70] examined the effect of biaxial strain on oxygen diffusivity using combined density functional theory (DFT) calculations and kinetic Monte Carlo simulations and concluded that bond reconfiguration poses an upper limit to the effect of epitaxial strain in enhancing the conductivity by expanding the conduction path.

A potential problem with these models is that they tackle the issue of epitaxial strain by stressing bulk structure (i.e., they do not explicitly include the presence of interfaces, which may incorporate interesting ingredients related to the chemical and structural compatibility of the merging lattices). Density-functional calculations have been used to investigate the influence of the (001)-oriented interface on the conductivity increase in YSZ/STO superlattices explicitly considering the presence of the interface by introducing mixed YSZ/STO supercells.[69] The authors of that work proposed that the combination of epitaxial strain and oxygen sublattice incompatibility between the two structures are key in yielding the highly conducting interface. They reported that 7% strain produces a drastic change in the O sublattice of YSZ, which becomes as disordered as expected from an increase in temperature up to 2000 K. The O ion mean square displacement (mobility) is strongly enhanced (by a factor of over 10^6) as a result of the combined presence of oxygen vacancies and disorder. The incompatibility of the oxygen positions in the interface planes (octahedral in STO versus tetrahedral in YSZ) are proposed to play a key role in stabilizing the highly conducting interface
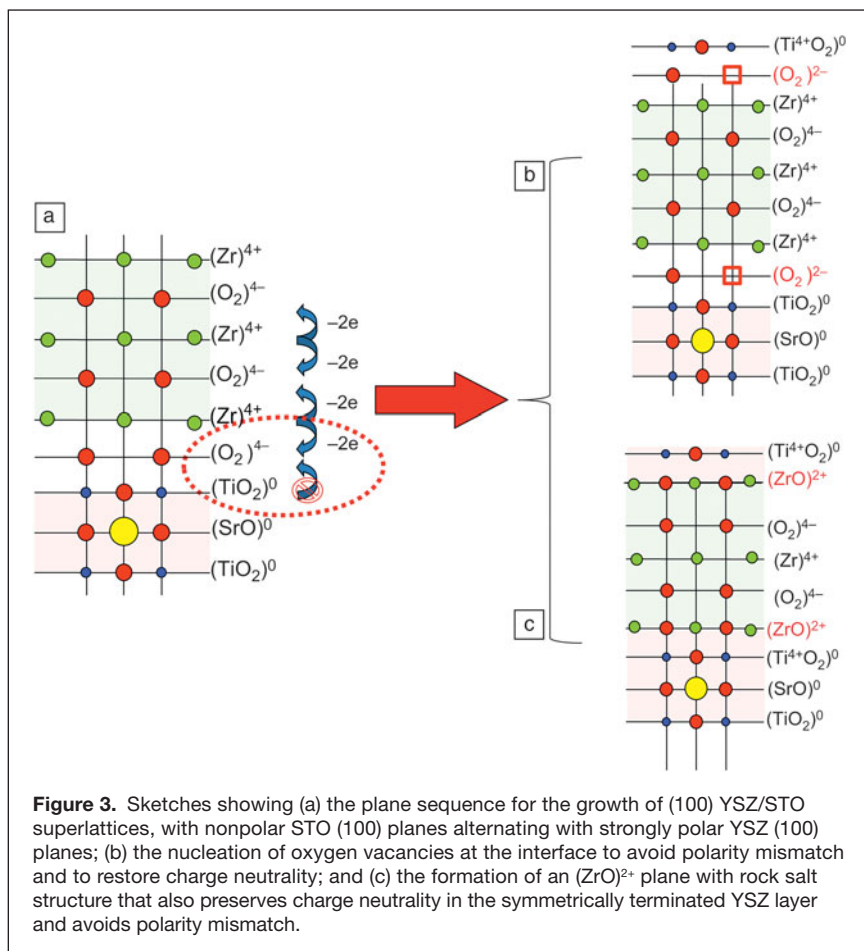
by introducing extreme disorder in the oxygen sublattice in the region close to the interface. Electron energy loss spectroscopy (EELS) experiments (both spectroscopy and imaging) have provided evidence for the oxygen disorder.[74] Moreover, density-functional simulations show that a new YSZ phase is stabilized in epitaxially strained heterostructures for mismatch strain levels in excess of 5.2%.[69] This result explains why these high levels of strain do not result in strain relaxation by mismatch dislocations and islanding, and provides evidence for the lattice relaxation playing a dominant role in phase stabilization.

Very recently, Li et al.[75] performed DFT and first-principles molecular dynamics simulations to examine the strain effect on oxygen conductivity in a $KTaO_3$/YSZ/$KTaO_3$ sandwich structure with 9.7% lattice mismatch. They found a large decrease in activation energy for ionic conduction, and estimated the oxygen ionic conductivity for KTO-strained zirconia to be 6.4×10^7 times higher than that of the unstrained bulk zirconia at 500 K. Interestingly, by using Al_2O_3 and $SrTiO_3$ instead of $KTaO_3$ in the simulations, a nearly linear relationship is identified between the energy barrier and the lattice mismatch in the sandwich structures in that work.

Atomic reconstruction at the interface

Aside from epitaxial strain, polarity mismatch may play an important role in determining the atomic reconstruction at the interface and may cause a departure from stoichiometry, which may be the source of increased density of (ionic) charge carriers. In the well-known case of the LAO/STO interface, the nonpolar STO (100) planes $((TiO_2)^0– (SrO)^0– (TiO_2)^0– \ldots)$ match the polar LAO (100) planes $((AlO_2)^-(LaO)^+– (AlO_2)^-\ldots)$, which causes a divergence in the electrostatic energy when the LAO thickness increases. In the polar catastrophe scenario,[76] electronic charge is transferred from the LAO surface to the interface, where Ti is partially reduced from 4+ to 3+, yielding a conducting interfacial state. This charge transfer process avoids the divergence of the electrostatic potential and identifies polarity mismatch as an important driving force in electronic reconstruction.[2–7,76]

It is worth noting that other processes have been proposed to originate the conducting state at the interface, such as formation of oxygen vacancies or intermixing, which might also originate at the polarity mismatch. There is also a strong polar discontinuity at the interfaces between ion conducting materials discussed in this work. For example, in the case of (100) YSZ/STO superlattices, the nonpolar STO (100) planes alternate with strongly polar YSZ (100) planes with a sequence $(Zr)^{4+}– (O_2)^{4+}(Zr)^{4+}– \ldots$. This plane sequence is the source of a very energetically unstable situation, which cannot be settled by electron transfer to the interface in the case of symmetric TiO_2-terminated STO interfaces shown by experiment[14] (see **Figure 3**a). An interesting possibility is that oxygen vacancies nucleate at the interface (one oxygen vacancy per every interface unit cell) to avoid polarity mismatch and to restore charge neutrality (see Figure 3b). This may be an additional

Figure 3. Sketches showing (a) the plane sequence for the growth of (100) YSZ/STO superlattices, with nonpolar STO (100) planes alternating with strongly polar YSZ (100) planes; (b) the nucleation of oxygen vacancies at the interface to avoid polarity mismatch and to restore charge neutrality; and (c) the formation of an $(ZrO)^{2+}$ plane with rock salt structure that also preserves charge neutrality in the symmetrically terminated YSZ layer and avoids polarity mismatch.

epitaxial interfaces, which may be important to understand modified ionic conductivity.

Oxygen surface exchange

Finally, a different scenario where oxide interfaces have recently shown their potential in connection with new materials for energy applications is oxygen exchange. In current SOFCs, if the conductance of the electrolyte is increased, either by increasing its conductivity or by reducing its thickness, electrode polarization losses become the dominant cause in limiting device performance.[79] The slow kinetics of the thermally activated oxygen reduction reaction at the cathode is responsible for a good part of the resistive losses of current oxide fuel cells and is in fact one of the factors critically limiting their operation at lower temperatures.[80] At the cathode, O_2 from the air is reduced, and O^{2-} cations are transported through the electrolyte to the anode where they react with the gaseous fuel, releasing electrons to the external circuit. The use of mixed electronic-ionic cathode materials along with surface treatments[81] and optimization of the surface microstructure[82,83] has resulted in one order of magnitude enhancement of the exchange activity.

Epitaxial strain has been revealed to be a very effective parameter in accelerating oxygen exchange,[84,85] and its role in surface chemistry and ion exchange has been a recent focus of great interest. First-principles calculations have shown that epitaxial strain favors oxygen vacancy formation in $LaCoO_3$,[86] a well-studied fuel cell cathode, as well as results in enhanced oxygen mobility.[87] Sase et al.[88] have shown that oxygen surface exchange in the $La_{0.6}Sr_{0.4}CoO_3/(La, Sr)_2 CoO_4$ heterointerface is increased by three orders of magnitude as compared to single cobaltite surfaces. The result is interpreted in terms of enhanced mobility at the interface connected with local strains. Jalili et al.[89] have shown that quite significant chemical modifications occur at the surface of $La_{0.7}Sr_{0.3}MnO_3$ epitaxial films resulting from strain, namely Sr enrichment and enhanced oxygen vacancy formation. Using tracer diffusion experiments with isotopically modified ^{18}O, Kubicek and collaborators[90] have evidenced faster surface exchange (by a factor of 4) and enhanced surface diffusion (by a factor of 10) in tensile strained $La_{1-x}Sr_xCoO_{3-\delta}$ layers grown on STO as compared to compressively strained ones grown on LAO. These effects are due to enhanced (oxygen) diffusion through reduced activation barriers for diffusion and/or energy (enthalpy) for oxygen vacancy formation.[90] Also, very recently, Prinz et al. found a fivefold increase in the oxygen surface exchange coefficient of single-crystal YSZ on optimizing the dopant concentration at the surface with the help of atomic layer deposition of a

source (other than the incompatibility between perovskite and the fluorite unit cell) to justify the nucleation of a large number of oxygen vacancies at YSZ/STO interfaces. Another possibility is the formation of a $(ZrO)^{2+}$ plane with a rock salt structure, as proposed recently by Dyer et al.[77] from theoretical arguments (see Figure 3c). This interface termination is consistent with experimental observations and also preserves charge neutrality in the symmetrically terminated YSZ layer and avoids polarity mismatch. This reconstruction may in fact be related to the proposed zirconate interfacial compound proposed recently by Cavallaro and collaborators.[78]

In a related context, Ramanathan et al.[53] have shown, from molecular dynamics simulations, that in YSZ films on MgO substrates, there is a slight enrichment of dopant (i.e., yttrium at the YSZ free surface compared to the YSZ–MgO interface), and the extent of dopant enrichment is greater for lower thickness YSZ films. As a result, the interfacial conductivity increases by two orders of magnitude as the YSZ film size decreases from 9 to 3 nm, owing to a decrease in activation energy barrier from 0.54 to 0.35 eV in the 1200–2000 K temperature range. In summary, apart from epitaxial strain, atomic reconstruction arising at interfaces as the result of polarity mismatch or other forms of chemical incompatibility may be the source of modified coordination and stoichiometry at

5–10 nm YSZ layer.[91] The results demonstrate the potential of oxide interface engineering between an electrolyte and electrode to optimize the performance of SOFCs or other electrochemical devices.

Summary and outlook

An interesting new facet of oxide interfaces has been recently uncovered in connection with materials for energy applications. The enhanced ionic conductivity found in heterostructures involving solid electrolytes may impact the performance of oxide-based energy generation and storage devices. In particular, they could provide an avenue to reduce the high operation temperatures of current solid oxide fuel cells, which impose severe constraints on materials selection and durability of devices compromised by thermal fatigue. The important limiting factors are the oxygen conductivity through the electrolyte and the oxygen exchange rate at the electrodes, both of which can be drastically improved at oxide interfaces. Epitaxial growth of the heterostructures seems to play an important role in determining the increase in the ionic conductivity. While there is solid evidence for enhanced ion mobility in epitaxial oxide ultrathin layers or interfaces, a polycrystalline structure or non-homogeneous strain distribution seems to suppress this enhancement. However, the ultimate reason for the enhanced conduction at oxide interfaces remains to be elucidated, and different scenarios have been proposed as being relevant to explain experimental data: (1) charge transfer and space-charge effects, (2) effect of epitaxial strain in opening diffusion paths, and (3) interface atomic reconstruction in stabilizing new phases with increased carrier concentration.

These experimental findings have also triggered a growing theoretical effort aimed at understanding the enhanced conductivity in strained layers. It is important to confront the results of the models that explicitly consider the presence of the interface with those examining the effect of modified bulk structures. Ultimately, understanding the mechanism underlying enhanced ion diffusivity at oxide interfaces should help in selecting suitable materials and designing appropriate nanostructures for future energy devices based on oxide nanolayers.

Acknowledgments

References

1. E. Dagotto, *Science* **309**, 257 (2005).
2. A. Ohtomo, H.Y. Hwang, *Nature* **427**, 423 (2004).
3. N. Reyren, S. Thiel, A.D. Caviglia, L. Fitting Kourkoutis, G. Hammerl, C. Richter, C.W. Schneider, T. Kopp, A.-S. Ruetschi, D. Jaccard, M. Gabay, D.A. Muller, J.-M. Triscone, J. Mannhart, *Science* **317**, 1196 (2007).
4. A. Brinkman, M. Huijben, M. van Zalk, J. Huijben, U. Zeitler, J.C. Maan, W.G. van derWiel, G. Rijnders, D.H.A. Blank, H. Hilgenkamp, *Nat. Mater.* **6**, 493 (2007).
5. E. Bousquet, M. Dawber, N. Stucki, C. Lichtensteiger, P. Hermet, S. Gariglio, J.M. Triscone, P. Ghosez, *Nature* **452**, 732 (2008).
6. S. Okamoto, A. Millis, *Nature* **428**, 630 (2004).
7. J. Mannhart, D.G. Schlom, *Science* **327**, 1607 (2010).
8. Y. Tokura, N. Nagaosa, *Science* **288**, 462 (2000).
9. S. Okamoto, A.J. Millis, *Nature* **428**, 630 (2004).
10. J. Chakhalian, J.W. Freeland, G. Strajer, J. Strempfer, G. Khaliullin, J.C. Cezar, T. Charlton, R. Dalgliesh, C. Bernhard, G. Cristiani, H.U. Habermeier, B. Keimer, *Nat. Phys.* **2**, 244 (2006).
11. P. Yu, J.-S. Lee, S. Okamoto, M.D. Rossell, M. Huijben, C.-H. Yang, Q. He, J.X. Zhang, S.Y. Yang, M.J. Lee, Q.M. Ramasse, R. Erni, Y.-H. Chu, D.A. Arena, C.-C. Kao, L.W. Martin, R. Ramesh, *Phys. Rev. Lett.* **105**, 027201 (2010).
12. J. Garcia-Barriocanal, J.C. Cezar, F.Y. Bruno, P. Thakur, N.B. Brookes, C. Utfeld, A. Rivera-Calzada, S.R. Giblin, J.W. Taylor, J.A. Duffy, S.B. Dugdale, T. Nakamura, K. Kodama, C. Leon, S. Okamoto, J. Santamaria, *Nat. Commun.* **1**, 82 (2010).
13. J. Garcia-Barriocanal, F.Y. Bruno, A. Rivera-Calzada, Z. Sefrioui, N.M. Nemes, M. Garcia-Hernandez, J. Rubio-Zuazo, G.R. Castro, M. Varela, S.J. Pennycook, C. Leon, J. Santamaria, *Adv. Mater.* **22**, 627 (2010).
14. J. Garcia-Barriocanal, A. Rivera-Calzada, M. Varela, Z. Sefrioui, E. Iborra, C. Leon, S.J. Pennycook, J. Santamaria, *Science* **321**, 676 (2008).
15. B.C.H. Steele, A. Heinzel, *Nature* **414**, 345 (2001).
16. A.S. Aricò, P. Bruce, B. Scrosati, J.M. Tarascon, W. van Schalkwijk, *Nat. Mater.* **4**, 366 (2005).
17. A.V. Chadwick, *Nature* **408**, 926 (2000).
18. T.H. Etsell, S.N. Flengas, *Chem. Rev.* **70**, 339 (1970).
19. J. Maier, *Solid State Ionics* **175**, 7 (2004).
20. R. Waser, M. Aono, *Nat. Mater.* **6**, 833 (2007).
21. H.L. Tuller, *Solid State Ionics* **131**, 143 (2000).
22. J. Maier, *Nat. Mater.* **4**, 805 (2005).
23. K.L. Kliewer, J.S. Koehler, *Phys. Rev.* **140**, 1226A (1965).
24. J. Maier, *J. Electrochem. Soc.* **134**, 1524 (1987).
25. H.L. Tuller, *Solid State Ionics* **131**, 142 (2000).
26. J. Maier, *Solid State Ionics* **157**, 327 (2003).
27. Y.M. Chiang, E.B. Lavik, I. Kosacki, H.L. Tuller, J.Y. Ying, *J. Electroceram.* **1**, 7 (1997).
28. N. Sata, K. Eberman, K. Eberl, J. Maier, *Nature* **408**, 946 (2000).
29. I. Kosacki, T. Suzuki, V. Petrovsky, H.U. Anderson, *Solid State Ionics* **136**, 1225 (2000).
30. C. Peters, A. Weber, E. Ivers-Tiffee, H. Störmer, D. Gerthsen, M. Bockmeyer, R. Krüger, "Interaction Between Grain Size and Electrical Conductivity in YSZ Thin Films," 2006 Fall Meeting, Materials Research Society (Boston, MA), AA10.3.
31. P. Mondal, H. Hahn, *Ber. Bunsen Ges. Phys. Chem.* **101**, 1765 (1997).
32. S. Jiang, *J. Mater. Res.* **12**, 2374 (1997).
33. G. Knoener, K. Reinemann, R. Roewer, U. Soedervall, H.-E. Schaefer, *Proc. Nat. Acad. Sci. U.S.A.* **100**, 3870 (2003).
34. R.A. De Souza, M.J. Pietrovski, U. Anselmi-Tamburini, S. Kim, Z.A. Munir, M. Martín, *Phys. Chem. Chem. Phys.* **10**, 2067 (2008).
35. S.J. Litzelman, J.L. Hertz, W. Jung, H. Tuller, *Fuel Cells* **5**, 294 (2008).
36. B.C.H. Steele, *Eur. Fuel Cell News* **7**, 16 (2000).
37. I. Kosacki, B. Gorman, H.U. Anderson, in *Ionic and Mixed Conductors, Vol. III*, T.A. Ramanayanaran, W.L. Worrell, H.L. Tuller, A.C. Kandkar, M. Morgensen, W. Gopel, Eds. (Electrochemical Society, Pennington, NJ, 1998), p. 631.
38. I. Kosacki, C.M. Rouleau, P.F. Becker, J. Bentley, D.H. Lowdness, *Solid State Ionics* **176**, 1319 (2005).
39. A. Karthikeyan, Ch.L. Chan, L. Ramanathan, *Appl. Phys. Lett.* **89**, 183116 (2006).
40. X. Guo, E. Vasco, S. Mi, K. Szot, E. Wachsman, R. Waser, *Acta Mater.* **53**, 5161 (2005).
41. S. Azad, O.A. Marina, C.M. Wang, L. Saraf, V. Shutthanandan, D.E. McCready, A. El-Azab, J.E. Jaffe, M.H. Englehard, C.H.F. Peden, S. Thevuthasan, *Appl. Phys. Lett.* **86**, 131906 (2006).
42. C.M. Wang, M.H. Englehard, S. Azad, L. Saraf, O.A. Marina, D.E. McCready, V. Shutthanandan, Z.Q. Yu, S. Thevuthasan, M. Watanabe, D.B. Williams, *Solid State Ionics* **177**, 1299 (2006).
43. A. Peters, C. Korte, D. Hesse, N. Zakharov, J. Janek, *Solid State Ionics* **178**, 67 (2007).
44. C. Korte, A. Peters, J. Janek, D. Hesse, N. Zakharov, *Phys. Chem. Chem. Phys.* **10**, 4623 (2008).
45. A. Ohtomo, D.A. Muller, J.L. Grazul, H. Hwang, *Nature* **419**, 378 (2002).
46. S. Thiel, G. Hammerl, A. Schmehl, C.W. Schneider, J. Mannhart, *Science* **313**, 1942 (2006).
47. X. Guo, *Science* **324**, 465 (2009).
48. J. Garcia-Barriocanal, A. Rivera-Calzada, M. Varela, Z. Sefrioui, E. Iborra, C. Leon, S.J. Pennycook, J. Santamaria, *Science* **324**, 465 (2009).
49. J. Garcia-Barriocanal, A. Rivera-Calzada, M. Varela, Z. Sefrioui, M.R. Diaz-Guillen, K.J. Moreno, J.A. Diaz-Guillen, E. Iborra, A.F. Fuentes, S.J. Pennycook, C. Leon, J. Santamaria, *ChemPhysChem* **10**, 1003 (2009).

50. E. Lee, F.B. Prinz, W. Cai, *Phys. Rev. B* **83**, 052301 (2011).
51. K.L. Ngai, *J. Non-Cryst. Solids* **203**, 232 (1996).
52. S.K.R.S. Sankaranarayanan, S. Ramanathan, *J. Chem. Phys.* **134**, 064703 (2011).
53. K.L. Ngai, J. Santamaria, C. Leon, *Eur. Phys. J. B* **86**, 7 (2013).
54. S.T. Norberg, S. Hull, I. Ahmed, S.G. Eriksson, D. Marrocchelli, P.A. Madden, P. Li, J.T.S. Irvine, *Chem. Mater.* **23**, 1356 (2011).
55. M. Sillassen, P. Eklund, N. Pryds, E. Johnson, U. Helmersson, J. Bottiger, *Adv. Funct. Mater.* **20**, 2071 (2010).
56. N. Schichtel, C. Korte, D. Hesse, J. Janek, *Phys. Chem. Chem. Phys.* **11**, 3043 (2009).
57. J. Jiang, X. Hu, W. Shen, C. Ni, J.L. Hertz, *Appl. Phys. Lett.* **102**, 143901 (2013).
58. B. Li, J. Zhang, T. Kaspar, V. Shutthanandan, R.C. Ewing, J. Lian, *Phys. Chem. Chem. Phys.* **15**, 1296 (2013).
59. J. Hyodo, S. Ida, J.A. Kilner, T. Ishihara, *Solid State Ionics* **230**, 16 (2013).
60. H. Aydin, C. Korte, M. Rohnkea, J. Janek, *Phys. Chem. Chem. Phys.* **15**, 1944 (2013).
61. S.P.S. Badwal, M.J. Bannister, M.J. Murray, *J. Electroanal. Chem.* **168**, 363 (1984).
62. D. Pergolesi, E. Fabbri, S.N. Cook, V. Roddatis, E. Traversa, J.A. Kilner, *ACS Nano* **6**, 10524 (2012).
63. M. Gerstl, G. Friedbacher, F. Kubel, H. Hutter, J. Fleig, *Phys. Chem. Chem. Phys.* **15**, 1097 (2013).
64. A. Cavallaro, M. Burriel, J. Roqueta, A. Apostolidis, A. Bernardi, A. Tarancón, R. Srinivasan, S.N. Cook, H.L. Fraser, J.A. Kilner, D.W. McComb, J. Santiso, *Solid State Ionics* **181**, 592 (2010).
65. A. Rivera-Calzada, M.R. Diaz-Guillen, O.J. Dura, G. Sanchez-Santolino, T.J. Pennycook, R. Schmidt, F.Y. Bruno, J. Garcia-Barriocanal, Z. Sefrioui, N.M. Nemes, M. Garcia-Hernandez, M. Varela, C. Leon, S.T. Pantelides, S.J. Pennycook, J. Santamaria, *Adv. Mater.* **23**, 5268 (2011).
66. E. Fabbri, D. Pergolesi, E. Traversa, *Sci. Technol. Adv. Mater.* **11**, 054503 (2010).
67. J.L.M. Rupp, *Solid State Ionics* **207**, 1 (2012).
68. C. Korte, N. Schichtel, D. Hesse, J. Janek, *Monatsh. Chem.* **140**, 1069 (2009).
69. T.J. Pennycook, M.J. Beck, K. Varga, M. Varela, S.J. Pennycook, S.T. Pantelides, *Phys. Rev. Lett.* **104**, 115901 (2010).
70. A. Kushima, B. Yildiz, *J. Mater. Chem.* **20**, 4809 (2010).
71. G. Dezenneau, J. Hermet, B. Dupe, *Int. J. Hydrogen Energy* **37**, 8081 (2012).
72. R.A. De Souza, A. Ramadan, S. Hörner, *Energy Environ. Sci.* **5**, 5445 (2012).
73. J. Hintenberg, T. Zacherle, R.A. de Souza, *Phys. Rev. Lett.* **110**, 2015901 (2013).
74. T.J. Pennycook, M.P. Oxley, J. Garcia-Barriocanal, F.Y. Bruno, C. Leon, J. Santamaria, S.T. Pantelides, M. Varela, S.J. Pennycook, *Eur. Phys. J. Appl. Phys.* **54**, 33507 (2011).
75. F. Li, R. Lu, H. Wu, E. Kan, C. Xiao, K. Deng, D.E. Ellis, *Phys. Chem. Chem. Phys.* **15**, 2692 (2013).
76. N. Nakagawa, H.Y. Hwang, D.A. Muller, *Nat. Mater.* **5**, 204 (2006).
77. M.S. Dyer, G.R. Darling, J.B. Claridge, M.J. Rosseinsky, *Angew. Chem. Int. Ed.* **51**, 3418 (2012).
78. A. Cavallaro, M. Burriel, J. Roqueta, A. Apostolidis, A. Bernardi, A. Tarancón, R. Srinivasan, S.N. Cook, H.L. Fraser, J.A. Kilner, D.W. McComb, J. Santiso, *Solid State Ionics* **13–14**, 592 (2010).
79. E.D. Wachsman, K.T. Lee, *Science* **334**, 935 (2011).
80. J. Fleig, *Annu. Rev. Mater. Res.* **33**, 361 (2003).
81. M. Kubicek, A. Limbeck, T. Frömling, H. Hutter, J. Fleig, *J. Electrochem. Soc.* **158**, B727 (2011).
82. S.B. Adler, *Chem. Rev.* **104**, 4791 (2004).
83. C. Peters, A. Weber, E. Ivers-Tiffee, *J. Electrochem. Soc.* **155**, B730 (2008).
84. M. Burriel, G. Garcia, J. Santiso, J.A. Kilner, J.C.C. Richard, S.J. Skinner, *J. Mater. Chem.* **18**, 416 (2008).
85. H.I. Ji, J. Hwang, K.J. Yoon, J.W. Son, B.K. Kim, H.W. Lee, J.H. Lee, *Energy Environ. Sci.* **6**, 116 (2013).
86. A. Kushima, S. Yip, B. Yildiz, *Phys. Rev. B* **11**, 115435 (2010).
87. J.W. Han, B. Yildiz, *J. Mater. Chem.* **21**, 18983 (2011).
88. M. Sase, K. Yasgiro, K. Sato, J. Mizusaki, T. Kawada, N. Sakai, K. Yamaji, T. Horita, H. Yokokawa, *Solid State Ionics* **178**, 1843 (2008).
89. H. Jalili, J.W. Han, Y. Kuru, Z. Cai, B. Yildiz, *J. Phys. Chem. Lett.* **2**, 801 (2011).
90. M. Kubicek, Z. Cai, W. Ma, B. Yildiz, H. Hutter, J. Fleig, *ACS Nano* **7**, 3276 (2013).
91. C.C. Chao, J.S. Park, X. Tian, J.H. Shim, T.M. Gür, F.B. Prinz, *ACS Nano* **7**, 2186 (2013). □

5 THINGS TO KNOW ABOUT

MRS Communications
The Letters and Prospectives Journal

For more information about MRS Communications,
visit **www.mrs.org/mrc** or email **mrc@mrs.org.**

For manuscript submission instructions,
visit **www.mrs.org/mrc-instructions.**

1 *MRS Communications* is publishing high-quality, rigorously reviewed materials science communications within **14 days of acceptance**.

2 *MRS Communications* received its **first Impact Factor** (IF) from the 2012 Thomson Science Citation Index (SCI) Journal Citation Reports® in record time—based upon only the first published issue and just one year of citations. Watch for our building success in 2014!

3 *MRS Communications* offers an **Open Access** publication option with, for a limited time only, a reduced article processing charge.

4 *MRS Communications* is a digital journal. Readers enjoy a **variety of access options** including mobile format, dynamic page-turning edition, and iTunes and Android apps.

5 *MRS Communications* has published high-impact papers in its first three volumes. Look for each new issue at www.journals.cambridge.org/mrc. **Prospectives articles**, a unique feature of this journal, include:

Materials processing strategies for colloidal quantum dot solar cells: advances, present-day limitations, and pathways to improvement
Graham H. Carey, Kang W. Chou, Buyi Yan, Ahmad R. Kirmani, Aram Amassian, Edward H. Sargent

Hairy nanoparticle assemblies as one-component functional polymer nanocomposites: opportunities and challenges
Nikhil J. Fernandes, Hilmar Koerner, Emmanuel P. Giannelis, Richard A. Vaia

Recent developments in ductile bulk metallic glass composites
Michael Ferry, Kevin Laws, Christopher White, David Miskovic, Karl Shamlaye, Wangiang Xu, Olga Biletska

Catalytic polymeric nanoreactors: more than a solid supported catalyst
Pepa Cotanda, Nikos Petzetakis, Rachel K. O'Reilly

Spectroscopic imaging in PFM: new opportunities for studying polarization dynamics in ferroelectrics and multiferroics
Rama Krishnan Vasudevan, Stephen Jesse, Yunseok Kim, Amit Kumar, Sergei V. Kalinin

Biomaterials-based strategies for the engineering of mechanically active soft tissues
Zhixiang Tong and Xinqiao Jia

MRS MATERIALS RESEARCH SOCIETY®

CAMBRIDGE UNIVERSITY PRESS